1-1-2015

PU.1 opposes IL-7-dependent proliferation of developing b cells with involvement of the direct target gene bruton tyrosine kinase

Darah A. Christie
Schulich School of Medicine & Dentistry

Li S. Xu
Schulich School of Medicine & Dentistry

Shereen A. Turkistany
Schulich School of Medicine & Dentistry

Lauren A. Solomon
Schulich School of Medicine & Dentistry

Stephen K.H. Li
Schulich School of Medicine & Dentistry

See next page for additional authors

The Journal of Immunology

PU.1 Opposes IL-7–Dependent Proliferation of Developing B Cells with Involvement of the Direct Target Gene *Bruton Tyrosine Kinase*

Darah A. Christie, Li S. Xu, Shereen A. Turkistany, Lauren A. Solomon, Stephen K. H. Li, Edmund Yim, Ian Welch, Gillian I. Bell, David A. Hess and Rodney P. DeKoter

J Immunol 2015; 194:595-605; Prepublished online 10 December 2014;
doi: 10.4049/jimmunol.1401569
http://www.jimmunol.org/content/194/2/595

The Journal of Immunology is published twice each month by
The American Association of Immunologists, Inc.,
1451 Rockville Pike, Suite 650, Rockville, MD 20852

Print ISSN: 0022-1767 Online ISSN: 1550-6606.

PU.1 Opposes IL-7–Dependent Proliferation of Developing B Cells with Involvement of the Direct Target Gene *Bruton Tyrosine Kinase*

Darah A. Christie,*[,1] Li S. Xu,*[,1] Shereen A. Turkistany,* Lauren A. Solomon,* Stephen K. H. Li,* Edmund Yim,* Ian Welch,[†] Gillian I. Bell,[‡,§] David A. Hess,[‡,§,¶] and Rodney P. DeKoter*[,¶]

Deletion of genes encoding the E26 transformation-specific transcription factors PU.1 and Spi-B in B cells (CD19-CreΔPB mice) leads to impaired B cell development, followed by B cell acute lymphoblastic leukemia at 100% incidence and with a median survival of 21 wk. However, little is known about the target genes that explain leukemogenesis in these mice. In this study we found that immature B cells were altered in frequency in the bone marrow of preleukemic CD19-CreΔPB mice. Enriched pro–B cells from CD19-CreΔPB mice induced disease upon transplantation, suggesting that these were leukemia-initiating cells. Bone marrow cells from preleukemic CD19-CreΔPB mice had increased responsiveness to IL-7 and could proliferate indefinitely in response to this cytokine. Bruton tyrosine kinase (BTK), a negative regulator of IL-7 signaling, was reduced in preleukemic and leukemic CD19-CreΔPB cells compared with controls. Induction of PU.1 expression in cultured CD19-CreΔPB pro–B cell lines induced *Btk* expression, followed by reduced STAT5 phosphorylation and early apoptosis. PU.1 and Spi-B regulated *Btk* directly as shown by chromatin immunoprecipitation analysis. Ectopic expression of BTK was sufficient to induce apoptosis in cultured pro–B cells. In summary, these results suggest that PU.1 and Spi-B activate *Btk* to oppose IL-7 responsiveness in developing B cells. ***The Journal of Immunology*****, 2015, 194: 595–605.**

Development of B lymphocytes proceeds through a series of steps marked by Ig gene rearrangement as well as ordered expression of transcription factors (1). Aberrant expression of various transcription factors can predispose developing B cells to leukemia (2). Development of B cell progenitors requires signaling through the IL-7R (3, 4). Productive rearrangement of the *IgH* locus in pro–B cells permits expression of IgH protein and assembly with surrogate L chain components to promote cell surface expression of a pre-BCR. Signaling through the pre-BCR promotes cell cycle exit and differentiation into small pre–B cells that initiate *Ig* κ or λ L chain rearrangement (5, 6). Completion of functional *Ig* L chain rearrangement enables differentiation into B cells expressing a functional BCR.

Several lines of evidence suggest that pre-BCR signaling and IL-7 signaling are mutually antagonistic. IL-7 signaling in pro–B/pre–B cells impairs *Igκ* rearrangement in a STAT5-dependent manner (7). Pre–B cells are released from the differentiation block induced by IL-7 by moving from microenvironments containing high IL-7 concentrations to low IL-7 concentrations (5, 8). Pre-BCR signaling interferes with the IL-7 signaling pathway using a mechanism that requires B cell linker protein (BLNK/SLP-65) (9). Finally, upon differentiation into immature B cells, the *Il7r* gene is permanently downregulated at the transcriptional level using mechanisms that are as yet uncharacterized (10). In summary, functional opposition of the pre-BCR and IL-7 signaling pathways is required for differentiation of large pre–B cells into small pre–B cells and *Ig* L chain rearrangement. Mutations in genes that impair this functional opposition can lead to loss of genomic integrity and leukemia (5).

PU.1 and Spi-B are highly related transcription factors of the E26 transformation–specific family. PU.1 and Spi-B are both expressed in developing B cells and have functional redundancy, likely interacting with a similar set of binding sites in the genome (11, 12). Mutations in *SPI1* encoding PU.1 are associated with relapsed B cell acute lymphoblastic leukemia (B-ALL) (13). Repression of the gene encoding Spi-B (*Spib*) was recently found to be associated with human precursor B-ALL (14) as well as with a mouse model of B-ALL (15). Our laboratory showed that combined null mutation of *Spi1* and *Spib* in mice ($CD19^{+/Cre}Spi1^{lox/lox}Spib^{-/-}$ mice, called CD19-CreΔPB mice in this study) leads to B-ALL at a median age of 21 wk at 100% incidence (16). The tumor sup-

*Centre for Human Immunology, Department of Microbiology and Immunology, University of Western Ontario, London, Ontario N6A 5C1, Canada; [†]Department of Animal Care and Veterinary Services, University of Western Ontario, London, Ontario N6A 5C1, Canada; [‡]Robarts Research Institute, University of Western Ontario, London, Ontario N6A 5C1, Canada; [§]Department of Physiology and Pharmacology, University of Western Ontario, London, Ontario N6A 5C1, Canada; and [¶]Division of Genetics and Development, Children's Health Research Institute, Lawson Research Institute, London, Ontario N6C 2R5, Canada

[1]D.A.C. and L.S.X. contributed equally to this study.

Received for publication June 20, 2014. Accepted for publication November 4, 2014.

This work was supported by Canadian Institutes of Health Research Grant MOP-106581 (to R.P.D.), a grant from the Leukemia and Lymphoma Society of Canada (to R.P.D.), and by an Ontario Graduate Scholarship (to S.K.H.L.).

The sequences presented in this article have been submitted to the Gene Expression Omnibus (http://www.ncbi.nlm.nih.gov/geo/) under accession numbers GSE48891 and GSE 58128.

Address correspondence and reprint requests to Dr. Rodney P. DeKoter, Department of Microbiology and Immunology, Schulich School of Medicine and Dentistry, University of Western Ontario, London, ON N6A 5C1, Canada. E-mail address: rdekoter@uwo.ca

The online version of this article contains supplemental material.

Abbreviations used in this article: ΔB, $CD19^{+/+}Spi1^{lox/lox}Spib^{-/-}$; B-ALL, B cell acute lymphoblastic leukemia; BM, bone marrow; BTK, Bruton tyrosine kinase; CD19-CreΔPB, $CD19^{+/Cre}Spi1^{lox/lox}Spib^{-/-}$; ChIP, chromatin immunoprecipitation; ChIP-seq, chromatin immunoprecipitation sequencing; NSG, NOD/SCID/$\gamma c^{-/-}$; qPCR, quantitative PCR; RT-qPCR, reverse transcription–quantitative PCR; WT, wild-type.

pressor gene *Blnk* is a direct target of activation by PU.1 and/or Spi-B (17). However, it is not clear how reduced PU.1 and Spi-B predispose developing B cells to malignant transformation in CD19-CreΔPB mice.

Bruton tyrosine kinase (BTK) is a tyrosine kinase that is critically required for pre-BCR/BCR signaling, and when inactivated by mutation, it is the most frequent cause of human X-linked agammaglobulinemia (18, 19). Mutation of *Btk* in mice is not sufficient to induce leukemia. However, mutation of *Btk* strongly synergizes with mutation of *Blnk* (SLP-65) in mice to induce leukemia in mice with ~75% incidence by 16 wk of age (20). Therefore, *Blnk* and *Btk* function as cooperating tumor suppressors in developing mouse B cells.

In the present study, we investigated the developmental origins and mechanisms of leukemogenesis in CD19-CreΔPB mice. Bone marrow (BM) pro–B cells were increased in frequency in preleukemic CD19-CreΔPB mice, and they were leukemia-initiating cells as determined by transplantation analysis. Bone marrow cells from preleukemic CD19-CreΔPB mice had increased responsiveness to IL-7 in culture that correlated with loss of BTK expression. Induction of PU.1 expression in cultured CD19-CreΔPB pro–B cells induced *Btk* expression, reduced STAT5 phosphorylation, and led to early apoptosis. PU.1 and Spi-B regulate *Btk* directly as shown by chromatin immunoprecipitation analysis. Finally, ectopic expression of BTK was sufficient to induce apoptosis in cultured CD19-CreΔPB pro–B cells. Taken together, these results suggest that PU.1 and Spi-B activate *Btk* to oppose IL-7 responsiveness in developing B cells.

Materials and Methods

Breeding and care of mice

Breeding and genotyping of $CD19^{+/Cre}Spi1^{lox/lox}Spib^{-/-}$ (referred to as CD19-CreΔPB) mice and $CD19^{+/+}Spi1^{lox/lox}Spib^{-/-}$ (referred to as ΔB) mice were performed as previously described (16). NOD/SCID/$\gamma c^{-/-}$ (NSG) mice were maintained in a barrier unit at the Western University Animal Care Facility. NSG mice received 300 cGy radiation 2 h before receiving a tail vein injection. C57BL/6 mice were purchased from Charles River Laboratories (Saint-Constant, QC, Canada). Mouse care was monitored under an approved animal use subcommittee protocol in accord with the Western University Council on Animal Care.

Cell culture

B-ALL or BM cells were cultured in IMDM (Cellgro; Corning, Manassas, VA) containing 5% IL-7–conditioned medium from the J558L-IL-7 cell line (21), 10% FBS (BioLogos, Mongomery, IL), 1× penicillin/streptomycin/L-glutamine (Lonza, Shawinigan, QC, Canada), and 5×10^{-5} M 2-ME (Sigma-Aldrich, St. Louis, MO). Retroviral vectors encoding Tet3G and inducible 3XFLAGPU.1 were produced as previously described (22). Inducible cell lines were maintained in medium containing 0.5 μg/ml puromycin (BioBasic, Markham, ON, Canada). All cell lines were maintained in 5% CO_2 atmosphere and 37°C.

PCR and genotyping

Relative frequencies of mRNA transcripts were measured by reverse transcription–quantitative PCR (RT-qPCR) and were normalized to the frequency of *Gapdh* transcripts using the comparative threshold cycle method (23). For chromatin immunoprecipitation (ChIP) experiments, relative frequencies of DNA fragments were measured by qPCR performed using a Rotor-Gene 6000 instrument (Corbett Life Sciences, Valencia, CA). Amplification of Ig rearrangements was performed as described by Cobaleda et al. (24). All primer sequences are described in Supplemental Table I.

Flow cytometry and immunoblotting

Flow cytometric analysis and sorting experiments were performed using FACSCalibur, LSR II, and FACSAria III instruments (BD Immunocytometry Systems, San Jose, CA). The purity of sorted cells was determined to be ≥98% upon reanalysis. Data were analyzed using FlowJo 9.1 software (Tree Star, Ashland, OR). Abs were purchased from eBioscience (San Diego, CA), BioLegend (San Diego, CA), or BD Biosciences (Mississauga, ON, Canada) and included PE-conjugated anti-CD19 (1D3), allophycocyanin– or BV421–anti-B220 (RA3-6B2), PE-Cy7–anti-IgM (II/41), PE–anti-CD93 (AA4.1), FITC–anti-CD23 (B3B4), FITC–anti-CD21 (eBio8D9), allophycocyanin–anti-CD24 (M1/69), PE–anti-CD93 (AA4.1), FITC– or PE–anti-BP-1 (6C3), biotin–anti-CD3 (145-2C11), allophycocyanin-Cy7– or allophycocyanin–anti-CD43 (1B11), FITC–anti-CD127 (A7R23), FITC–anti-CD45.1 (A20), PE-Cy5.5–anti-CD45.2 (clone 104), and allophycocyanin–annexin V. Staining of intracellular targets was performed using the Fix and Perm kit (Life Technologies, Burlington, ON, Canada) and Phosflow PE anti-pSTAT5 pY694 (BD Biosciences). Live/dead cell staining was performed with the Live/Dead fixable yellow dead cell stain kit (Life Technologies). For immunoblotting analysis whole-cell lysates from enriched splenic B cells were probed with anti-BTK Ab (Cell Signaling Technology, Whitby, ON, Canada), HRP goat anti-rabbit secondary Ab (Thermo Fisher), and visualized with SuperSignal West Pico reagent (Thermo Fisher).

Histological and microscopic analysis

Mice were euthanized by lethal i.p. injection of 540 mg/ml sodium pentobarbital (Euthanyl Forte, Bimeda-MTC Animal Health, Cambridge, ON, Canada). Tissues were fixed in 10% neutral buffered formalin. Femurs were decalcified for 96 h in 26% formic acid (TBD-2, Thermo Fisher, Pittsburgh, PA). Tissues were paraffin embedded, sectioned, and stained with H&E. High-resolution micrographs were captured using a Q-Color3 digital camera (Olympus, Markham, ON, Canada).

Microarray analysis

RNA was prepared from sorted cells using RNA-Bee (Tel-Test, Friendswood, TX). RNA integrity and purity were checked using a 2100 Bioanalyzer (Agilent Technologies, Santa Clara, CA). RNA was processed using the WT Terminal Labeling and Hybridization kit (Affymetrix, Santa Clara, CA) according to the manufacturer's instructions and analyzed using Mouse Exon 1.0 ST arrays (Affymetrix) at the London Regional Genomics Centre. Data analysis was performed using Partek Genomics Suite (Partek, St. Louis, MO). Batch effect removal was performed using ComBat software (25). Differentially expressed genes were identified using one-way ANOVA and a cut-off of 1.5-fold with $p < 0.05$. Heat maps and volcano plots were generated using Hierarchical Clustering Explorer. Partek Pathway software was used to identify biological pathways using the Kyoto Encyclopedia of Genes and Genomes database, and p values were calculated using a Fisher exact test. Microarray data are available from the Gene Expression Omnibus under accession no. GSE48891.

ChIP analysis

Mouse splenic B cells enriched by negative selection of CD43-expressing cells, cultured i660BM cells, or mouse WEHI-279 cells stably expressing 3XFLAG-tagged PU.1 or Spi-B were cross-linked with 1% formaldehyde for 10 min at room temperature. ChIP was performed as previously described (12) using anti-PU.1 (Santa Cruz Biotechnology), anti-FLAG (Sigma-Aldrich), or control mouse anti-IgG Ab (Santa Cruz Biotechnology) conjugated to protein G Dynabeads (Invitrogen, Burlington, ON, Canada). Enrichment was measured using qPCR of DNA immunoprecipitated with anti-PU.1 normalized to anti-IgG, using primers indicated in Supplemental Table I. Fold enrichment was calculated using the comparative threshold cycle method (23). For ChIP sequencing (ChIP-seq) analysis, chromatin solutions with an average DNA fragment size of ~200 bp were generated using a Bioruptor 300 waterbath sonicator (Diagenode, Sparta, NJ). DNA was quantified using a 2100 Bioanalyzer (Agilent Technologies). Libraries were generated using the Kapa HTP Library Preparation kit (Kapa Biosystems) as per the manufacturer's recommendations. Size selection was performed on a Pippin Prep instrument (Sage Biosciences). Libraries were quantified using the Quant-iT PicoGreen dsDNA assay kit (Life Technologies) and the Kapa Illumina GA with Revised Primers–SYBR Fast Universal kit (D-Mark). Average size fragments were determined using a LaChip GX (PerkinElmer) instrument. Libraries were sequenced on an SR100 run on a HiSeq 2000 (Illumina). Two independent ChIP-seq experiments were conducted for PU.1 and Spi-B. Peak finding and data analysis were performed using Galaxy Suite (26). Peaks were called using MACS version 1.0.1 (27) with a genome size of 1.9×10^9 bp (MM9) using input controls. Peaks were called with a tag size set to either 75 (rep1) or 100 (rep2), bandwidth of 300, and a p value cutoff for peak detection of 1×10^{-5}. Peak Model was generated using an mfold high-confidence enrichment ratio against background of 15. Wiggle files were created using a resolution of 10 bp. Independent experiments were combined and normalized to call consensus peaks using mmChIP v1.0.0 with a mappable genome size of 191×10^7 and a p value cutoff for peak detection of 1×10^{-5} (28). Input.bed

files for mmChip were generated using Convert from BAM to BED tool v0.1.0 in Galaxy. ChIP-sequence data are available from the Gene Expression Omnibus under accession no. GSE58128.

Statistical analysis

All data are reported as means ± SD. Statistical significance was determined using a Student *t* test on biological replicates unless otherwise indicated. Values with $p < 0.05$ were considered significant. Statistical analysis was performed using Prism 5.0 (Graphpad Software, La Jolla, CA).

Results

Increase in frequency of immature B cells in the BM of CD19-CreΔPB mice

Deletion of genes encoding PU.1 and Spi-B in B cells (CD19-CreΔPB mice) leads to impaired B cell development, followed by B-ALL at 100% incidence and with a median survival of 21 wk (16). However, the developmental origin of B-ALL in CD19-CreΔPB mice was not previously examined. BM B cell development was examined in detail using flow cytometry and the "Hardy" classification system of fractions A–F (29). Both wild-type (WT; C57BL/6) and ΔB (*Spib*$^{-/-}$) BM cells were included as controls because these two types of mice do not develop leukemia. First, BM cells were prepared from 6- to 10-wk-old WT, ΔB, or CD19-CreΔPB mice. Total B220^{+} BM cell frequencies were slightly increased in 6- to 10-wk-old ΔB mice but were decreased in 6- to 10-wk-old CD19-CreΔPB mice (Fig. 1A, 1C). Frequencies of B220^{lo}CD43^{-}IgM^{+} cells (fraction E immature B cells) were significantly increased in 6- to 10-wk-old ΔB and CD19-CreΔPB mice, whereas frequencies of B220^{hi}CD43^{-}IgM^{+} (fraction F mature recirculating B cells) were significantly decreased (Fig. 1A, 1D). Analysis of BM development was also performed in mice aged 11–18 wk. Total B220^{+} BM cell frequencies were dramatically decreased in 11- to 18-wk-old CD19-CreΔPB mice (Fig. 1E). Frequencies of fraction C pro–B cells and fraction E immature B cells were dramatically expanded, representing nearly 30 and 50%, respectively, of all B220^{+} cells in older CD19-CreΔPB mice (Fig. 1B, 1F). Frequencies of fraction F B cells were reduced even further in older mice, as previously reported for mature splenic B cells (16) (Fig. 1B, 1F). In conclusion, immature B cells were increased in frequency in the BM of adult CD19-CreΔPB mice preceding overt leukemia.

Enriched fraction C pro–B cells from BM of CD19-CreΔPB mice transfer disease

Increased frequencies of fraction C pro–B cells in CD19-CreΔPB mice suggested that these might represent leukemia-initiating

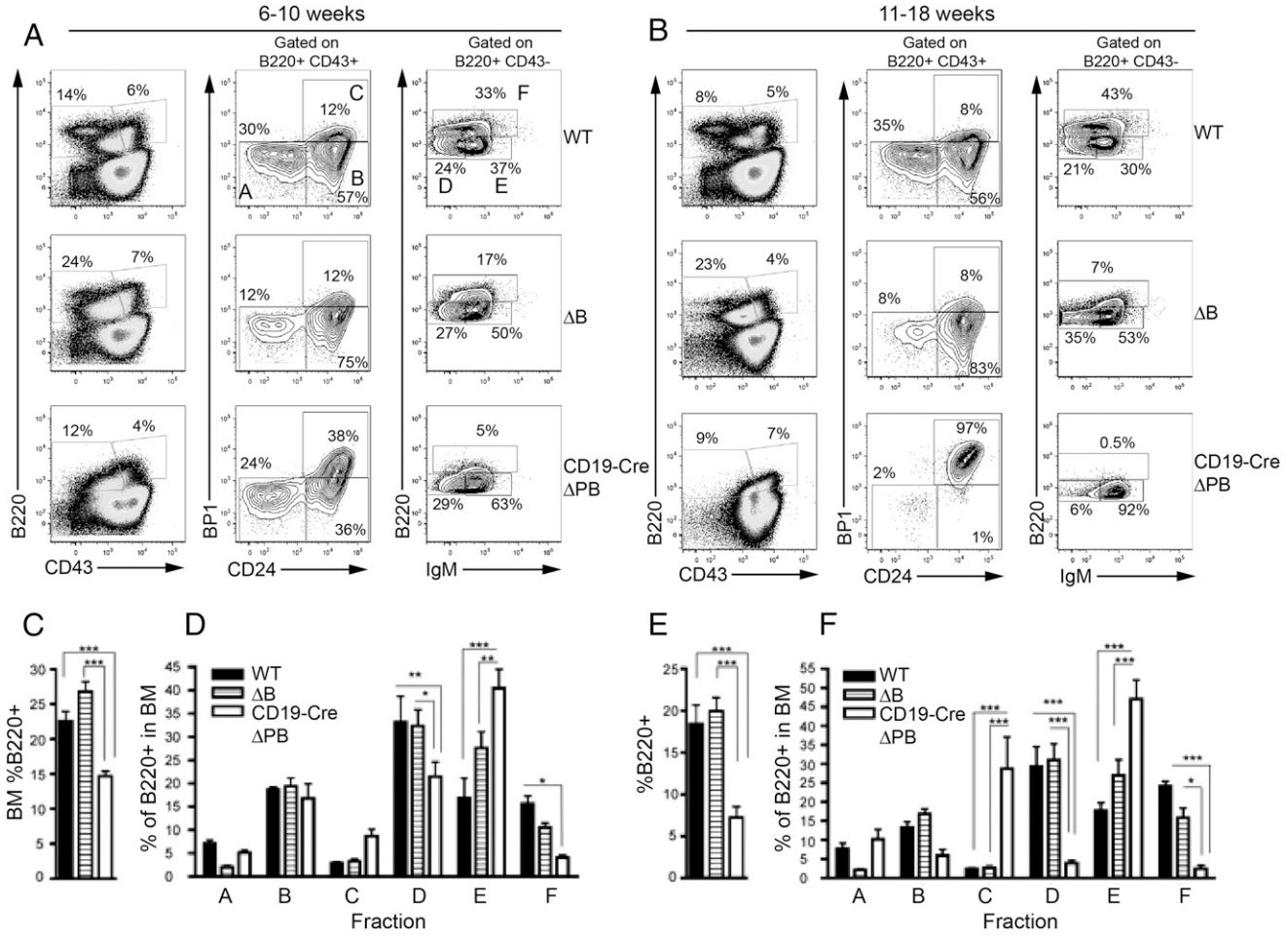

FIGURE 1. Alterations in the frequency of immature B cells in the BM of CD19-CreΔPB mice. (**A**) Representative frequencies of immature B cell (Hardy) fractions in BM of 6- to 10-wk-old CD19-CreΔPB mice. Markers used are indicated on the axes. The *top right two panels* indicate the identity of fractions A–F. Genotypes are indicated on the right. (**B**) Representative frequencies of immature B cell fractions in BM of 11- to 18-wk-old CD19-CreΔPB mice. Markers used are indicated on the axes. (**C**) Quantitation of BM B220^{+} B cell frequencies for groups of five mice of each indicated genotype aged 6–10 wk. Legend is shown in (**D**). (D) Quantitation of BM B cell fraction frequencies for groups of five mice of each indicated genotype aged 6–10 wk. Frequencies are expressed as the percentage of all B220^{+} BM cells. (**E**) Quantitation of BM B220^{+} B cell frequencies for groups of five mice of each indicated genotype aged 11–18 wk. Legend is shown in (D). (**F**) Quantitation of BM B cell fraction frequencies for groups of five mice of each indicated genotype aged 11–18 wk. Frequencies are expressed as the percentage of all B220^{+} BM cells. *$p < 0.05$, **$p < 0.01$, ***$p < 0.001$.

cells. To test this idea, transplantation experiments were performed using sorted cells from 6- to 10-wk-old ΔB (control) or CD19-CreΔPB mice. First, mature splenic B cells ($B220^+CD19^+CD93^-Ig\kappa^+$ cells) were enriched using cell sorting and injected i.v. into immunodeficient NSG mice (30). Recipient mice receiving 5×10^5 mature splenic B cells of either genotype showed no signs of illness until the experiment was terminated at 4 mo (Fig. 2A). Next, NSG mice were transplanted with 10^5 fraction C pro–B cells from ΔB or CD19-CreΔPB donors. Fraction C pro–B cells were enriched by cell sorting using the gating strategy shown in Fig. 1A. NSG mice injected with ΔB pro–B cells did not show signs of disease at any time point (Fig. 2B). In contrast, NSG mice receiving CD19-CreΔPB fraction C pro–B cells became ill and required euthanasia with a median time of 113.5 d (Fig. 2B). The spleens of NSG mice receiving CD19-CreΔPB fraction C pro–B cells contained high frequencies of leukemia cells expressing BP-1 and CD93 as determined by flow cytometry (Fig. 2C). Histopathological examination revealed that every tissue examined in NSG mice receiving CD19-CreΔPB pro–B cells was infiltrated with leukemia cells. Spleen and BM of transplanted NSG mice showed extensive infiltration of leukemia cells resulting in effacement of the normal architecture (Fig. 3A, 3B). Liver showed extensive infiltration of leukemia cells throughout the sinusoids with focal aggregates of leukemia cells in the portal and periportal regions (Fig. 3B, Supplemental Fig. 1A). The cortex of the brain showed meningeal invasion of leukemia cells (Fig. 3D, Supplemental Fig. 1B) whereas pancreatic tissues showed a large metastatic aggregate of leukemia cells (Fig. 3E). In conclusion, these results suggest that BM fraction C pro–B cells are leukemia-initiating cells in CD19-CreΔPB mice.

Analysis of gene expression in leukemic cells from CD19-CreΔPB mice reveals a pattern of impaired BCR signaling

Analysis of gene expression can provide important insights into pathways of oncogenic transformation (31). As a control for PU.1-dependent gene expression, cell sorting was used to enrich splenic $CD19^+B220^+$ B cells from the spleen of ΔB mice (Fig. 4A, *left panel*). For the experiment, cell sorting was used to enrich splenic $CD19^+B220^{lo}$ B-ALL cells or residual $CD19^+B220^+$ B cells from leukemic CD19-CreΔPB mice (Fig. 4A, *right panel*). RNA was prepared from sorted samples from these three groups and analyzed for gene expression using Affymetrix 1.0 ST exon arrays. Using a cutoff of a 1.5-fold change and p value of <0.05 by one-way ANOVA, 2908 genes were found to be downregulated and 3477 genes were upregulated in CD19-CreΔPB $CD19^+B220^{low}$ B-ALL cells compared with ΔB control cells. For the top 100 differentially expressed genes, downregulated genes were reduced by an average of 56-fold and upregulated genes increased by an average of 27-fold (Fig. 4B). Exon-specific analysis confirmed that the 3′ end of the *Spi1* transcript encoding PU.1 was reduced by an average of 20-fold in CD19-CreΔPB B-ALL cells, whereas the 5′ end was transcribed equivalently, as predicted by the Cre-mediated deletion of exons 4 and 5 in these mice (16). Gene expression was also compared with residual $CD19^+B220^+$ B cells from CD19-CreΔPB mice. Interestingly, these cells showed changes in gene expression that were intermediate between CD19-CreΔPB $CD19^+B220^{low}$ B-ALL cells and ΔB B cells (Fig. 4C). CD19-CreΔPB B cells expressed *Spi1* transcripts at levels intermediate between the other two populations, suggesting that these were B cells with delayed deletion of *Spi1* (Fig. 4C).

In the published literature at least 110 genes have been shown to be directly regulated by PU.1 using biochemical approaches (32). Of these 110 genes, 44 (40%) were downregulated in CD19-CreΔPB B-ALL cells compared with controls and 11 (10%) were upregulated. The remaining 55 genes (50%) were not significantly altered. Thus, 50% of known PU.1 target genes in this list were significantly altered in our study (Fig. 4D). Next, gene ontology analysis was performed. For genes that were upregulated in CD19-CreΔPB B-ALL cells compared with control ΔB B cells, the top two pathways as ranked by enrichment score and p value included cell cycle and DNA replication. Specific genes that were highly expressed in CD19-CreΔPB B-ALL cells and were confirmed by RT-qPCR included *Il7r* (encoding IL-7Rα), *Lgr5*, *Lef1*, *Enpep*

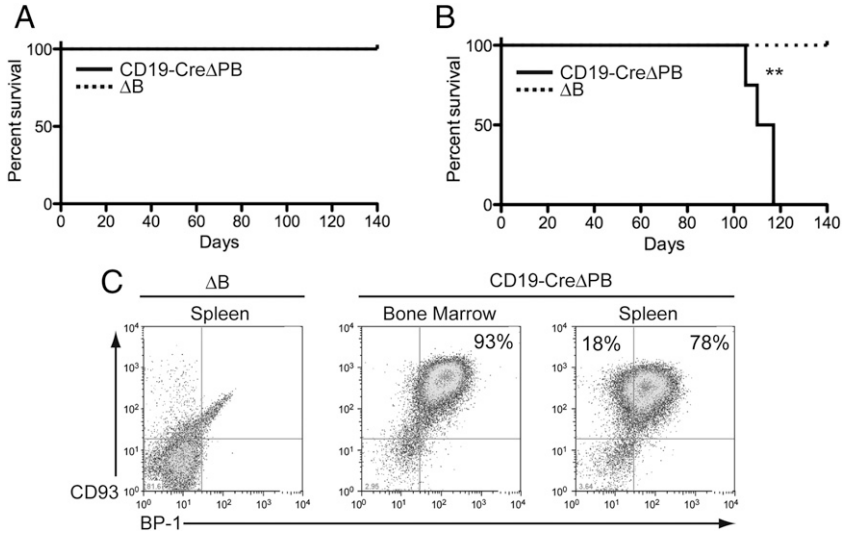

FIGURE 2. Purified fraction C cells from BM of 6-wk-old CD19-CreΔPB mice transfer disease to immunodeficient recipient mice. (**A**) Mature splenic B cells do not transfer disease. Mature B cells ($CD93^-B220^+CD19^+Ig\kappa^+$) were enriched from the spleen of 6-wk-old ΔB or CD19-CreΔPB mice by cell sorting. Sorted cells (5×10^5) were injected i.v. into sublethally irradiated (300 cGy) NSG mice (four per group). Mice were euthanized after 4 mo without signs of illness. (**B**) Fraction C pro–B cells ($B220^+CD24^+CD43^+BP\text{-}1^+$) were purified from the BM of 6-wk-old ΔB or CD19-CreΔPB mice by cell sorting. Sorted cells (1×10^5) were injected i.v. into sublethally irradiated (300 cGy) NSG mice (four mice per group). Mice were euthanized upon signs of illness. Median survival time of NSG mice transplanted with BM fraction C cells from CD19-CreΔPB mice was 113.5 d, significantly shorter than that for controls ($p \leq 0.01$ by Mantel–Cox log-rank test). (**C**) Representative flow cytometric analysis of leukemic mice. BM and spleen from transplanted mice were analyzed by flow cytometry using the indicated Abs. B-ALL cells were identified by cell surface expression of CD93 and BP-1. $^{**}p < 0.01$.

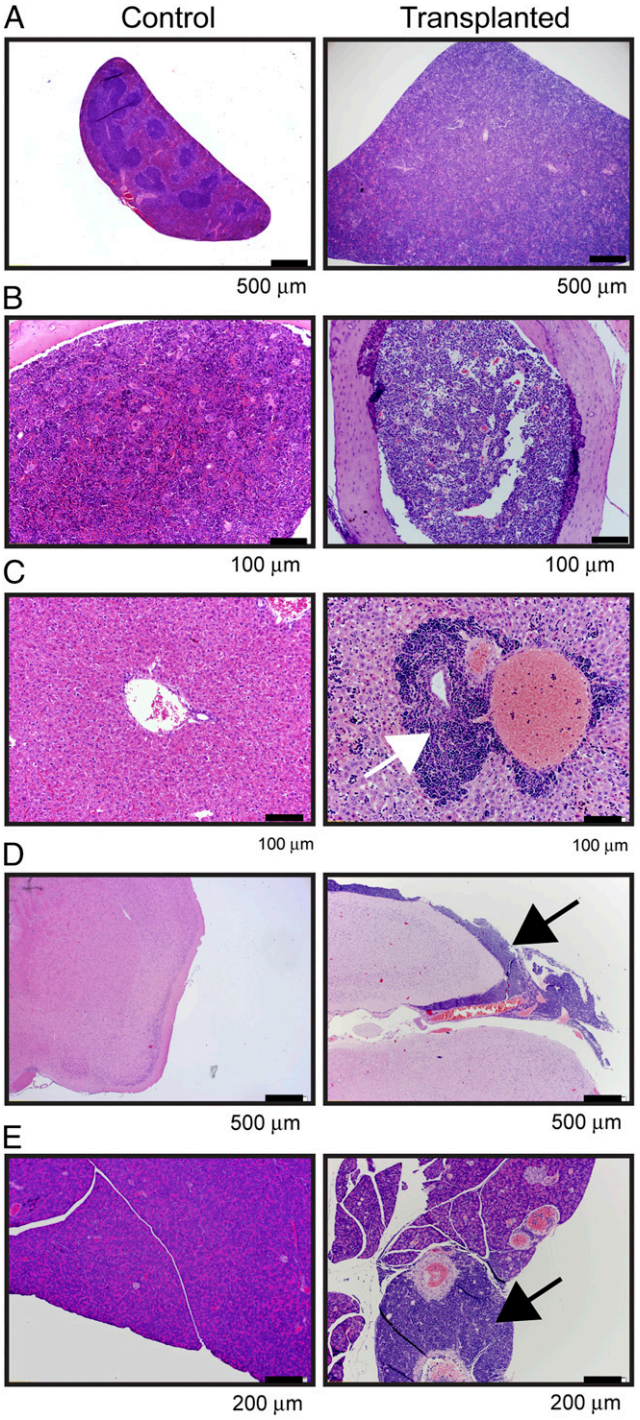

FIGURE 3. Leukemia-infiltrated tissues in transplanted NSG mice. Representative H&E-stained sections were photographed from four mice analyzed. *Left panels* show control C57BL/6 tissues for reference. *Right panels* show leukemia-infiltrated NSG tissues at low magnification. Scale bars are indicated for each panel. (**A**) Spleen. Control and NSG spleen cross-sections were photographed at an original magnification ×4. (**B**) BM. Decalcified femur cross-sections were photographed at an original magnification ×20. (**C**) Liver. Control and NSG mouse sections show liver triads of portal vein, artery, and bile duct. Original magnification ×20. (**D**) Brain. Control and NSG mouse sections show cortical sections in the dorsal–ventral orientation. Original magnification ×4. (**E**) Pancreas. Original magnification ×10.

(encoding BP-1), and *Tcfl2* (Fig. 4B, 4E). As expected based on differential B220 staining, *Ptprc* (encoding B220) was one of the most highly downregulated genes (Fig. 4B, 4E). Importantly, for genes that were downregulated in CD19-CreΔPB B-ALL cells compared with control ΔB B cells, the biological pathway with the lowest *p* value identified using gene ontology analysis was BCR signaling. A large number of genes in this biological pathway were significantly downregulated, including *Shp1*, *Syk*, *Lyn*, *Btk*, *Blnk*, *Vav*, *Rac*, *Bcap*, and *Grb2*. Several of these downregulated genes were confirmed by RT-qPCR analysis of three biological replicates (Fig. 4E). This analysis confirmed downregulation of *Blnk* (encoding B cell linker protein), *Lyn* (encoding the tyrosine kinase Lyn), and nearly 100-fold downregulation of *Btk* (encoding BTK) (Fig. 4B, 4E). Downregulation of *Btk* was greater when measured by RT-qPCR than when measured by microarray (Fig. 4E). In summary, analysis of gene expression in CD19-CreΔPB leukemia cells identified *Btk* and other key genes involved in BCR signaling as the most significantly downregulated in these cells.

Altered IL-7 responses in developing B cells from CD19-CreΔPB mice

IL-7Rα was among the most highly increased genes in our analysis (Fig. 4C, 4E). To determine whether immature B cells in the BM of preleukemic CD19-CreΔPB mice had altered responses to IL-7, unfractionated BM cells from 6- to 8-wk-old WT, ΔB, or CD19-CreΔPB mice were placed in culture with ST2 stromal cells and IL-7. Cell counts and passages were performed every 4 d until proliferation ceased. BM cells from ΔB and CD19-CreΔPB mice reproducibly generated more proliferating cells than did WT mice upon initial culture (representative experiment shown in Fig. 5A). Interestingly, ΔB and CD19-CreΔPB BM cells contained higher levels of phosphorylated STAT5 upon IL-7 restimulation than did WT BM cells (Supplemental Fig. 2). However, WT and ΔB cultures did not continue to proliferate after three passages. In contrast, BM cells from CD19-CreΔPB mice proliferated indefinitely and in all five trials could be readily established as cell lines (Fig. 5A). These results suggested that BM pro–B cells from CD19-CreΔPB mice had increased IL-7 sensitivity.

Mutation of *Btk* in mice has previously been shown to lead to increased IL-7 sensitivity in mouse BM cells (20, 33). Therefore, we determined whether *Btk* mRNA transcript levels correlated with *Spi1* mRNA transcript levels during the process of *Spi1* deletion under the control of CD19-Cre in cultured CD19-CreΔPB BM cells. RT-qPCR analysis was performed on RNA prepared from CD19-CreΔPB BM cells placed in culture with IL-7 and passaged up to eight times. At early passage numbers, cultured CD19-CreΔPB pro–B cells expressed high levels of B220 (Fig. 5B, *left panels*), *Spi1* transcripts (Fig. 5C), and *Btk* transcripts (Fig. 5E). After repeated passage, expression of B220, *Spi1*, and *Btk* were lost (Fig. 5B, *right panels*, 5C–E). *IL7r* transcripts increased on a per cell basis from passage 1 to passage 8 (Fig. 5D). Cell lines established from the BM of 6-wk-old CD19-CreΔPB mice expressed IL-7Rα, c-Kit, and CD19 (Fig. 5B, 5E). Proliferation of the cells was IL-7–dependent. Two of five cell lines had detectable *Igh* rearrangements (Fig. 5G). However, these cell lines did not express IgH on the cell surface. None of the five lines established had detectable *Igκ* rearrangements, or expressed Igκ protein on the cell surface. Therefore these cell lines resembled cultured pro–B cells rather than pre–B cells. In conclusion, the changes that occurred in cultured CD19-CreΔPB BM B cells during the process of *Spi1* deletion, including increased IL-7Rα expression, reduced B220 expression, and reduced BTK expression, were similar to differences between ΔB B cells and CD19-CreΔPB leukemia cells (Fig. 4). These changes might therefore occur in the BM of CD19-CreΔPB mice during the process of *Spi1* deletion and precede leukemic transformation.

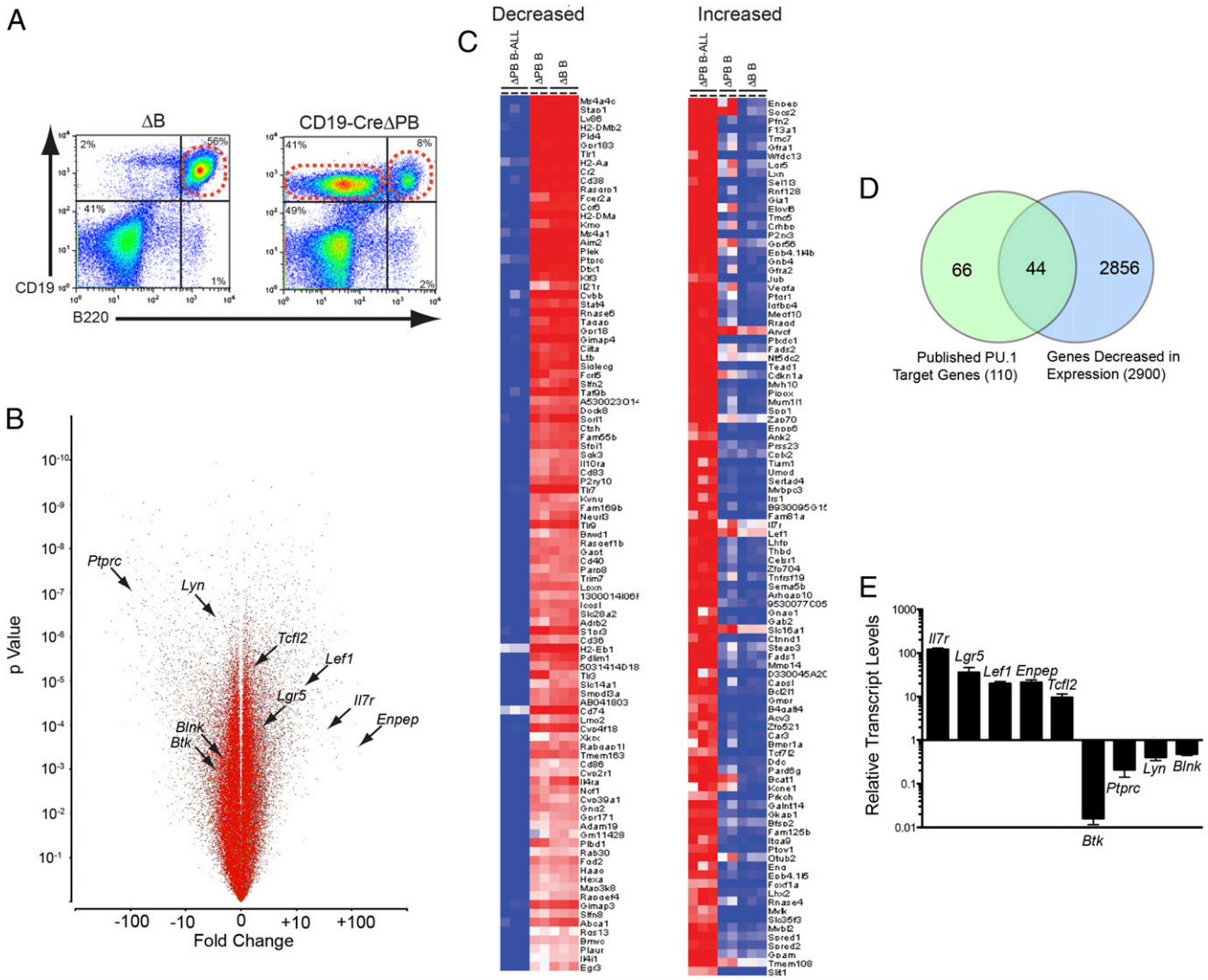

FIGURE 4. Gene expression analysis of CD19-CreΔPB leukemia suggests impaired BCR signaling. (**A**) Sort gates for splenic ΔB B cells and CD19-CreΔPB B-ALL cells. Three ΔB B cell samples, three CD19-CreΔPB B220^{lo}CD19^{+} B-ALL samples, and two CD19-CreΔPB B220^{+}CD19^{+} residual B cell samples were collected and analyzed individually by microarray. (**B**) Volcano plot of changes in gene expression in splenic CD19-CreΔPB B-ALL cells compared with ΔB B cells. Genes of interest are indicated by arrowheads. (**C**) Heat map comparing changes in gene expression in splenic CD19-CreΔPB B-ALL cells (ΔPB B-ALL), splenic CD19-CreΔPB B220^{+} B cells (ΔPB B), and ΔB B cells (ΔB B). The top 50 decreased genes are shown on the *left*; the top 50 increased genes are shown on the *right*. (**D**) Venn diagram showing overlap between published PU.1 target genes and genes downregulated in CD19-CreΔPB B-ALL cells compared with ΔB B cells. Of 110 published PU.1 target genes, 44 were significantly downregulated in CD19-CreΔPB B-ALL cells. (**E**) Confirmation of alternatively expressed mRNA transcripts. RT-qPCR was used to confirm relative upregulation of five indicated genes and down-regulation of four indicated genes in CD19-CreΔPB B-ALL cells compared with ΔB B cells. Error bars represent means and SD of three biological replicates and all had p values ≤ 0.05 by the Student t test.

PU.1 induces Btk *expression and loss of proliferation in cultured CD19-CreΔPB pro–B cells*

To determine the consequences of restoring PU.1 expression in CD19-CreΔPB cells, we made use of a doxycycline-inducible system (22). A BM-derived CD19-CreΔPB pro–B cell line, 660BM, was generated as described in Fig. 5. 660BM cells were IL-7–dependent and rapidly died by apoptosis when deprived of IL-7. 660BM cells were infected with a retroviral regulator vector encoding Tet3G and a retroviral response vector encoding PU.1 under the control of a Tet3G-responsive promoter (Fig. 6A). A clonal cell line termed i660BM was generated by picking a single GFP^{+} colony grown in methylcellulose containing IL-7 and puromycin. *Spi1* (encoding PU.1) expression could be highly induced in i660BM cells with concentrations of doxycycline as low as 70 ng/ml (Fig. 6B). Interestingly, 48 h after PU.1 induction, i660BM cells shrank in size as determined by reduced forward light scatter (Fig. 6C). Transition of high forward scatter to low forward scatter cells was doxycycline dose–dependent (Fig. 6D). All low forward scatter cells stained brightly with annexin V, indicating early apoptosis, whereas high forward scatter cells had low levels of annexin V staining (Fig. 6E). Induction of PU.1 in i660BM cells resulted in reduced STAT5 phosphorylation, suggesting that signaling downstream of the IL-7R was inhibited in these cells (Fig. 6F). In summary, these results show that induction of PU.1 reduced STAT5 phosphorylation, reduced cell size, and induced early apoptosis.

PU.1 and Spi-B directly regulate the Btk *gene*

The promoter region of *Btk* contains binding sites capable of interacting with PU.1 (34, 35). To determine whether PU.1 can induce BTK expression, we performed anti-BTK immunoblot analysis. Inducible i660BM cells did not express detectable BTK

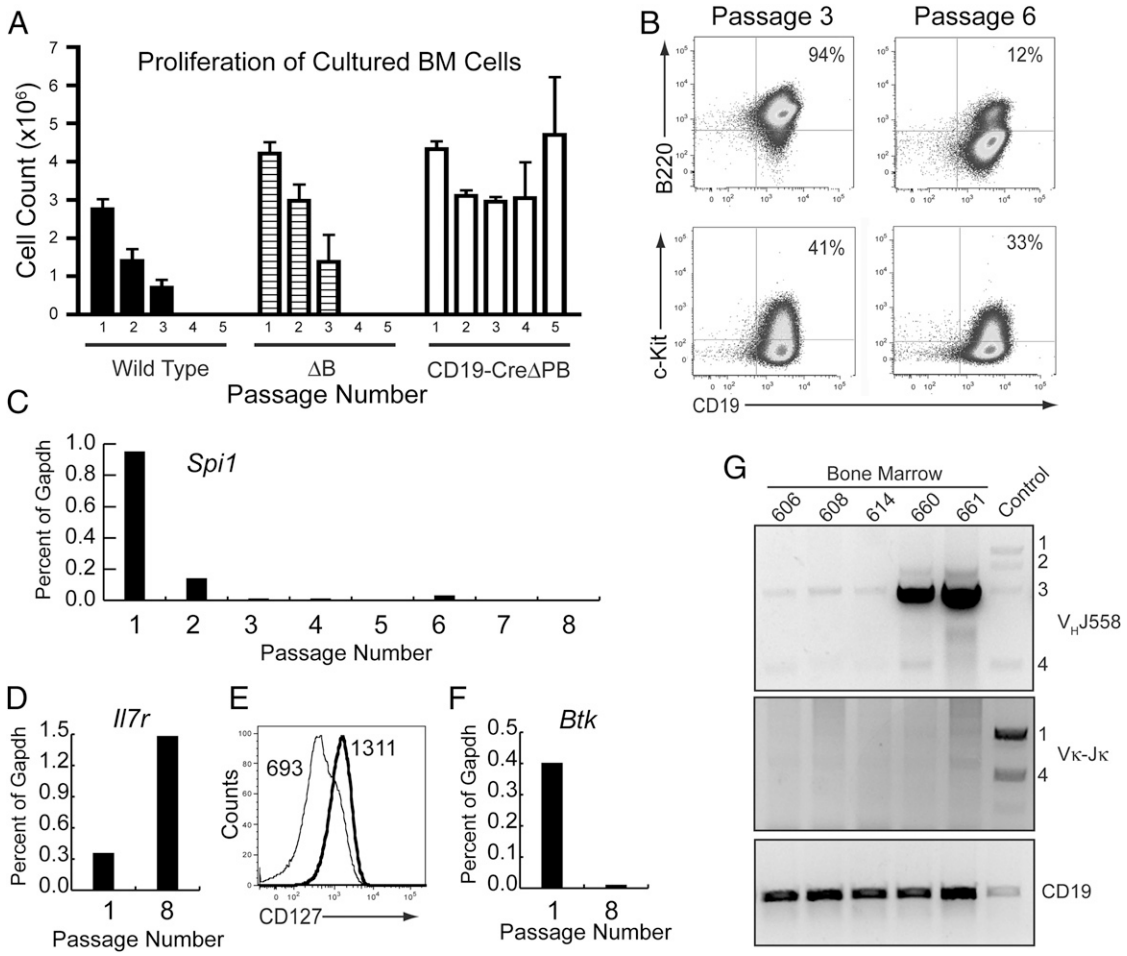

FIGURE 5. CD19-CreΔPB BM B cells have increased responsiveness to IL-7. (**A**) CD19Cre-ΔPB developing B cells proliferate indefinitely in response to IL-7. WT, ΔB, or CD19Cre-ΔPB BM cells from 6- to 10-wk-old mice of the indicated genotypes were cultured with IL-7 and ST2 stromal cells. Counts are shown at each passage after being initially established with 1 million cells. (**B**) B220 expression is downregulated upon passage of CD19Cre-ΔPB BM cells. Flow cytometric analysis was performed with the indicated Abs after three or six passages in IL-7 and ST2 cells. (**C**) *Spi1* transcripts (encoding PU.1) rapidly decline in cultured CD19Cre-ΔPB BM cells. (**D**) *Il7r* transcripts, encoding IL-7Rα, increase in frequency from passage 1 to 8. (**E**) Cultured CD19Cre-ΔPB BM cells express IL-7Rα on their surface. Passage 3 CD19Cre-ΔPB cells were stained and analyzed for IL-7Rα (CD127) using flow cytometry. Thin line indicates isotype control; thick line indicates CD127-stained cells. Numbers indicate mean fluorescence. (**F**) *Btk* transcripts, encoding BTK, decrease in frequency from passage 1 to 8. Results shown are one representative of three independent experiments. (**G**) Cultured CD19-CreΔPB BM–derived cell lines have undetectable *Igκ* rearrangements. PCR analysis was used to detect *Igh* (*upper panel*) or *Igκ* (*middle panel*) rearrangements from genomic DNA. Type of rearrangement is indicated on the *y*-axis. CD19 (*lower panel*) was used as a control. Control was a CD19-CreΔPB B-ALL of polyclonal origin. BM-derived cell line names are indicated on the *x*-axis.

protein when cultured without doxycycline. However, BTK was expressed after PU.1 induction (Fig. 7A). RT-qPCR measurement of gene expression showed that *Btk* mRNA transcripts were highly induced by PU.1 (Fig. 7B). To determine whether PU.1 directly regulates *Btk* in B cells, we performed anti-PU.1 ChIP experiments. In i660BM cells, interaction of PU.1 with the *Btk* promoter was inducible by doxycycline at 24 (Fig. 7C) and 48 h (Fig. 7D). In mouse splenic B cells, PU.1 was also found to interact with the *Btk* promoter as well as with the *Mef2c* enhancer as a positive control (Fig. 7E). Therefore, PU.1 was found to interact with the *Btk* promoter in both pro–B-like cells and mature B cells. For mouse Spi-B, no ChIP-quality Abs are currently available. Therefore, to determine whether Spi-B could also interact with the *Btk* promoter, we performed ChIP-seq analysis using anti-FLAG ChIP in 3× FLAG–tagged PU.1 or Spi-B–infected mouse WEHI-279 cells (L.A. Solomon, S.K.H. Li, J. Piskorz, L.S. Xu, and R.P. DeKoter, submitted for publication). Analysis of ChIP-seq data identified nearly identical peaks of PU.1 or Spi-B interaction near the annotated transcription start site of *Btk* (Fig. 7F). These data therefore indicate that *Btk* may be regulated by both PU.1 and Spi-B. To determine whether *Btk* expression requires PU.1 in vivo, we examined BTK protein levels by immunoblot of the few B cells that are present in the spleen of preleukemic CD19-CreΔPB mice. We found that BTK protein levels were reduced in CD19-CreΔPB B cells compared with either WT or ΔB B cells (Fig. 7G). Collectively, these results show that PU.1 and Spi-B can activate BTK expression in the B cell lineage.

Restoration of BTK expression was previously shown to induce apoptosis in cultured leukemia cells lacking BTK expression (36). To determine whether BTK was sufficient to induce apoptosis in cultured 660BM cells, these cells were infected with pMSCV-hBTK-FLAG retrovirus encoding BTK and GFP (37) or pMSCV-IRES-GFP alone as a control. Infection of 660BM cells with BTK induced early apoptosis by 48 h as determined by annexin V staining (Fig. 7H, 7I). We conclude that ectopic expression of BTK in 660BM cells is sufficient to induce early apoptosis.

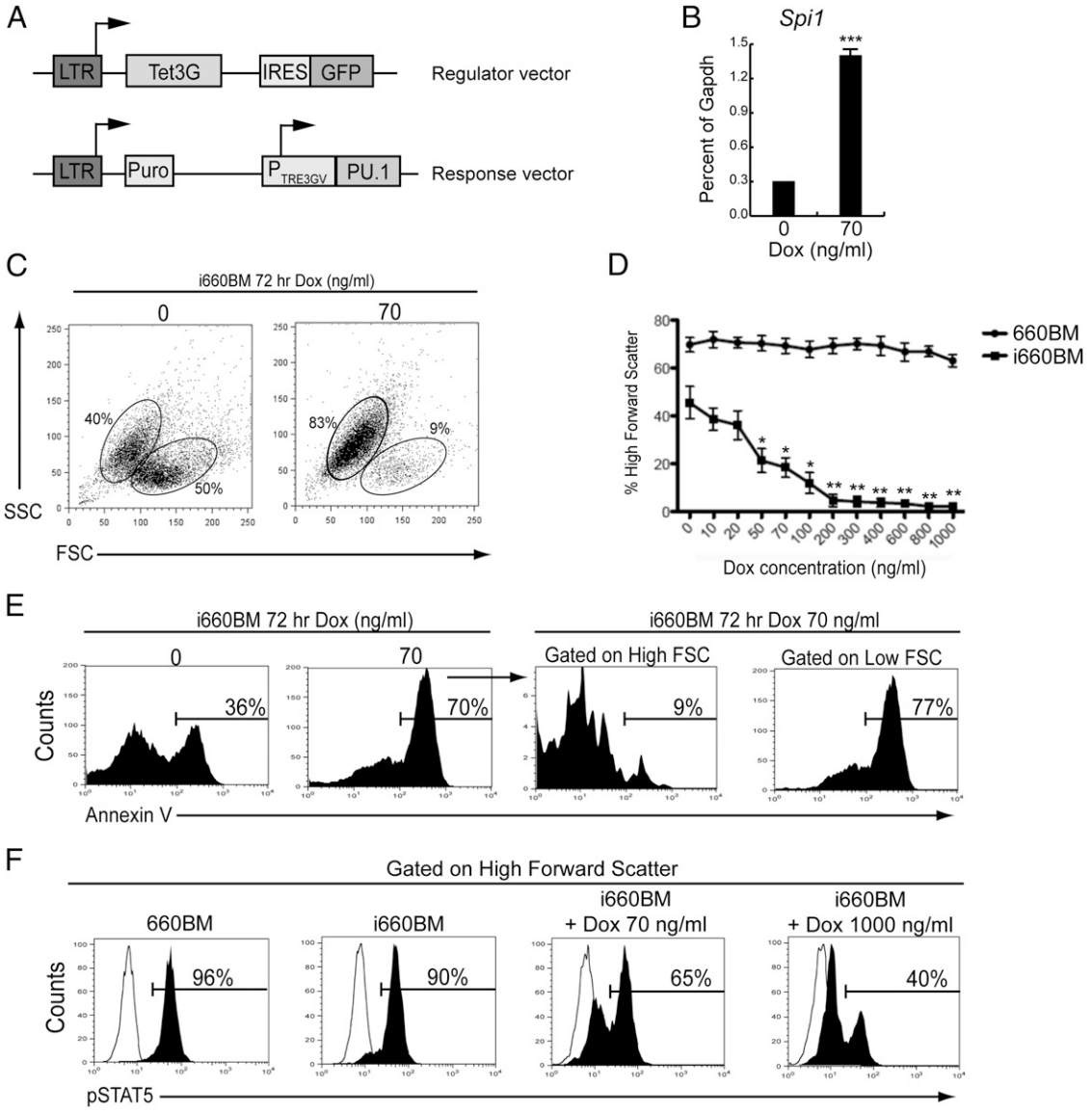

FIGURE 6. Induction of PU.1 expression induces early apoptosis in 660BM cells. (**A**) Schematic of retroviral vectors used in the inducible PU.1 system. The regulator vector encodes the Tet3G transactivator protein and GFP whereas the response vector encodes PU.1 and a puromycin resistance gene (Puro). (**B**) *Spi1* mRNA transcripts encoding PU.1 were induced after 48 h with doxycycline. *Spi1* transcript levels were determined using RT-qPCR and expressed as a percentage of steady-state control *Gapdh* mRNA transcripts. (**C**) Loss of high forward scatter i660BM cells upon 72 h of doxycycline induction. Flow cytometry was used to measure forward light scatter (*x*-axis) and side scatter (*y*-axis) after 72 h of doxycycline induction at the indicated concentrations. (**D**) Dose response of the percentage of high forward scatter cells (*y*-axis) compared with doxycycline concentration (*x*-axis). Flow cytometry was used to determine high forward scatter versus low forward scatter as shown in (C) 72 h after doxycycline induction. (**E**) Induction of early apoptosis. i660BM cells were cultured for 48 h in the presence of IL-7 and doxycycline at the indicated concentrations. Annexin V staining was quantified by flow cytometry. (**F**) Reduced STAT5 phosphorylation as a consequence of PU.1 induction. i660BM cells were cultured for 48 h in the presence of IL-7 and doxycycline at the indicated concentrations. After 48 h, STAT5 phosphorylation (pSTAT5) was quantified by flow cytometry. $*p < 0.05$, $**p < 0.01$, $***p < 0.001$ as determined by the Student *t* test compared with 0 ng/ml doxycycline.

Discussion

In the present study, we showed that deletion of the genes encoding PU.1 and Spi-B leads to an alteration of immature B cell frequencies in the BM. Enriched pro–B cells from 6- to 10-wk-old CD19-CreΔPB mice induced leukemia in transplanted recipients, suggesting that these were leukemia-initiating cells. Analysis of gene expression in B-ALL cells from CD19-CreΔPB mice showed that PU.1 and Spi-B enforce expression of many genes required for BCR signaling, including *Btk*. PU.1 was sufficient to induce *Btk* expression in a CD19-CreΔPB pro–B cell line. ChIP experiments demonstrate that *Btk* is directly activated by PU.1 and Spi-B. BTK expression was dramatically reduced in splenic B cells lacking PU.1 and Spi-B. Finally, ectopic expression of BTK was sufficient to induce apoptosis in cultured pro–B cells lacking PU.1 and Spi-B. Taken together, these results show that PU.1 and Spi-B are required for BTK expression in B cells, and reduced BTK expression as a consequence of PU.1/Spi-B deletion is associated with abnormal IL-7–dependent expansion of pro–B cells in the BM.

The present study showed that a key gene dramatically downregulated in B-ALL cells from CD19-CreΔPB mice was *Btk* (Fig. 6). *Btk* was previously implicated as a potential target gene of PU.1 (34, 35), a result that is now confirmed in this study. Our experiments demonstrated that PU.1 interacts directly with the *Btk* promoter in WEHI-279 cells and the pro–B cell line 660BM, and that Spi-B interacts with the *Btk* promoter in WEHI-279 cells. It remains to be determined whether Spi-B interacts with the *Btk*

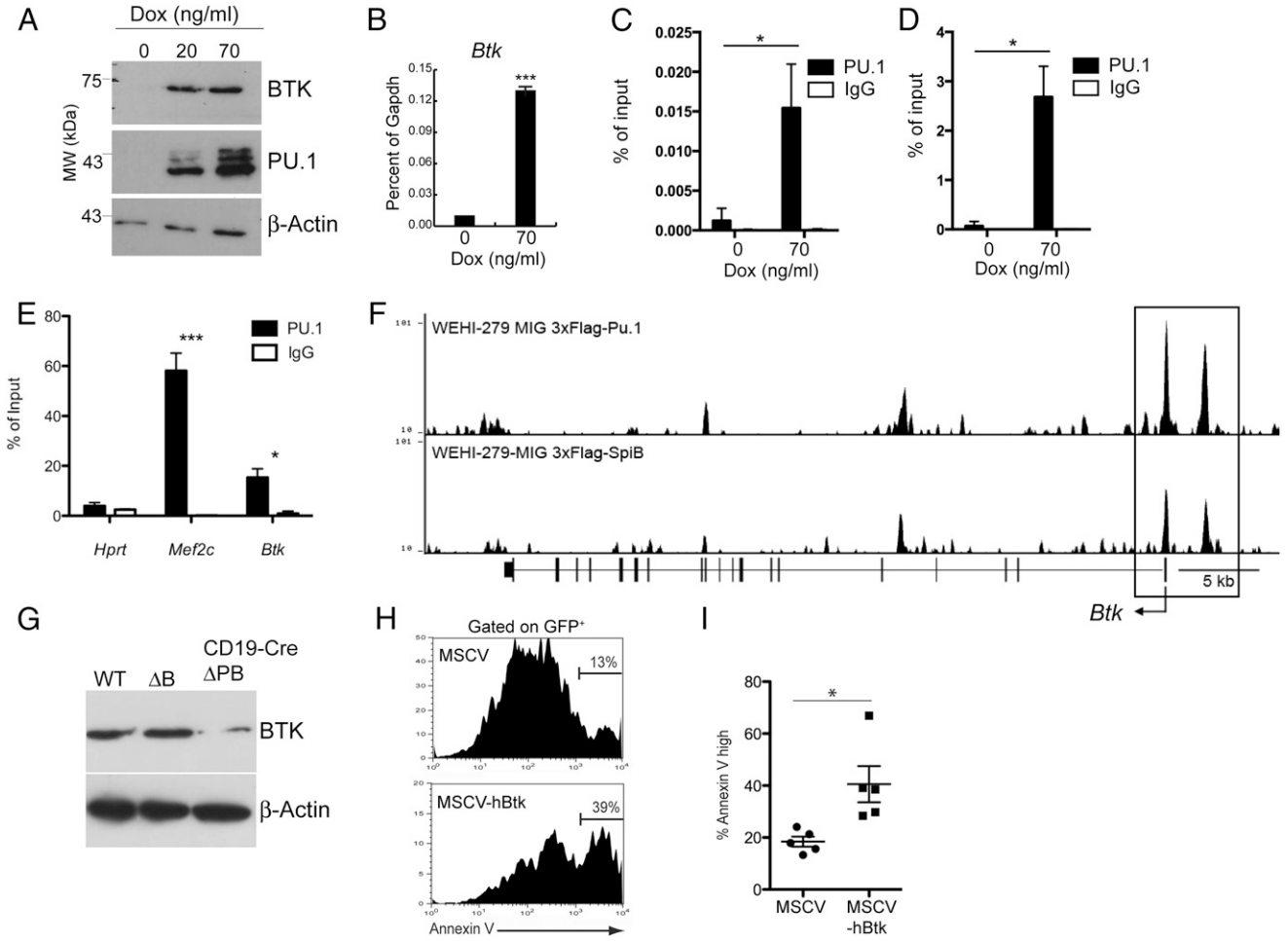

FIGURE 7. PU.1 and Spi-B directly activate transcription of *Btk*. (**A**) Induction of PU.1 and BTK protein by low concentration of doxycycline (Dox) in i660BM cells. Immunoblot using anti-BTK, anti-PU.1, or anti–β-actin Abs was performed on cells after 48 h of induction using the indicated concentrations of Dox. (**B**) *Btk* mRNA transcripts are induced by 48 h with Dox. *Btk* transcript levels were determined using RT-qPCR and are expressed as a percentage of steady-state control *Gapdh* mRNA transcripts. (**C** and **D**) ChIP analysis shows that PU.1 interacts directly with the *Btk* promoter in i660BM cells after Dox induction. ChIP was performed using anti-PU.1 or IgG (control) Abs and chromatin prepared from i660BM cells induced with 70 ng/ml Dox for 24 h (C) or 48 h (D). qPCR was used to quantify the *Btk* promoter in uninduced (0 ng/ml Dox) or induced (70 ng/ml Dox) cells. Statistical analysis was performed on technical replicates. (**E**) ChIP analysis shows that PU.1 interacts directly with the *Btk* promoter in mouse splenic B cells. ChIP was performed using anti-PU.1 or IgG (control) Abs and chromatin prepared from C57BL/6 mouse–enriched splenic B cells. qPCR was used to quantify the *Hprt* promoter as a negative control, *Mef2c* enhancer as a positive control, or the *Btk* promoter. (**F**) ChIP-seq analysis shows that both PU.1 and Spi-B interact with the *Btk* promoter in B cells. Murine WEHI-279 lymphoma cells expressing 3× FLAG–tagged PU.1 or Spi-B were analyzed by ChIP-seq. Peaks located within and near the *Btk* gene are shown. (**G**) Western blot showing reduced BTK expression in splenic B cells from 6- to 10-wk-old CD19Cre-ΔPB mice. Splenic B cells were enriched from mice of the indicated genotypes and immunoblotted with anti-BTK or anti–β-actin Abs. (**H**) Ectopic expression of BTK induces early apoptosis in cultured pro–B cells. 660BM cells were infected with the MSCV (control) or MSCV-hBTK (encoding BTK) retroviral vectors and analyzed after 48 h using flow cytometry for annexin V staining. The marker indicates the frequency of cells staining highly with annexin V. (**I**) Mean and SD of five biological replicate experiments. The *y*-axis indicates the frequency of annexin V^{hi} cells gated on GFP^+ infected 660BM cells. $*p < 0.05$, $***p < 0.001$ using a paired two-tailed *t* test.

promoter in pro–B cells. *Btk* gene expression was directly correlated with *Spi1* transcript levels in cultured CD19-CreΔPB BM cells during the process of *Spi1* deletion (Fig. 5C, 5E) consistent with the idea of this gene being PU.1-dependent. In contrast, *Btk* transcript levels inversely correlated with *Il7r* transcript levels (Figs. 4E, 5D) as well as with IL-7 responsiveness (Fig. 5A). Deletion of the *Btk* gene was previously shown to be sufficient to cause increased IL-7 responsiveness in BM pre–B cells (20). BTK is a key component of the pre-BCR signaling pathway that functions to block IL-7R signaling in developing B cells (38). We note that the 660BM cells used in our study resemble pro–B cells rather than pre–B cells based on their lack of expression of surface IgM or Igκ. Therefore, BTK may function to oppose IL-7R signaling in pro–B cells that do not yet express a pre-BCR or BCR. In summary, reduced BTK expression caused by deletion of PU.1 and/or Spi-B may be sufficient to explain why CD19-CreΔPB pro–B cells are hyperresponsive to IL-7 in culture. Increased responsiveness of CD19-CreΔPB pro–B/pre–B cells to IL-7 may also explain why fraction C pro–B cells expand in the BM of preleukemic mice.

Our laboratory previously showed that *Blnk* (encoding B cell linker protein) is a direct target of PU.1 and Spi-B in developing B cells (17). Loss-of-function mutation of *Btk* strongly synergizes with loss-of-function mutation of *Blnk* in mice to induce B-ALL in mice with ~75% incidence by 16 wk of age (20). BM cells from *Btk/Blnk* knockout mice have increased sensitivity to IL-7 and increased ability to proliferate in response to IL-7 (33, 39, 40). Similar to CD19-CreΔPB mice, leukemias from *Btk/Blnk* knock-

out mice express BP-1, CD43, and IL-7R and can be readily cultured as cell lines in response to IL-7 (9, 20). Taken together, these similarities suggest that reduced expression of both BLNK and BTK, as a consequence of PU.1 and Spi-B deletion, may explain why developing CD19-CreΔPB B cells are susceptible to malignant transformation. It is still not fully understood why reduced BTK and BLNK lead to leukemia in mice. It has been speculated that the mechanism might involve prolonged transit through the V(D)J recombination process, leading to accumulation of undesired mutations (41). Expression of an *Igh* transgene prevents leukemia in *Btk/Blnk* knockout mice, possibly because this accelerates transition through *Ig* recombination (41). We note that B-ALL cells from CD19-CreΔPB mice express high levels of RAG-1 and RAG-2 as determined by microarray analysis (11- and 9-fold higher than control cells, respectively). More investigation will be needed to determine whether ongoing *Ig* recombination in CD19-CreΔPB B cells plays a role in leukemic transformation.

To summarize, we propose a model to explain why deletion of PU.1 and Spi-B in the B cell lineage leads to impaired B cell development and eventually B-ALL. In CD19-CreΔPB mice, the *Spi1* gene is deleted starting at the pro–B cell stage under the control of CD19. Pro–B cells that delete *Spi1* downregulate expression of the target genes *Btk* and *Blnk*. Reduced BTK and BLNK expression would in turn result in increased IL-7R sensitivity, leading to increased proliferation of pro–B and large pre–B cells. Additionally, reduced BTK and BLNK might lead to delayed V(D)J recombination, leading to accumulation of mutations. Most cells that delete *Spi1* likely do not progress past the pre–B cell stage due to impaired BTK/BLNK-dependent pre-BCR signaling. We speculate that leukemia arises in rare progenitor cells from the late pro–B/early pre–B fraction C and C′ compartments.

There are a number of similarities between the CD19-CreΔPB mouse model of B-ALL and human precursor B-ALL. Mutations in *SPI1* encoding human PU.1 have been identified in relapsed precursor B-ALL (13), and repression of *SPIB* encoding human Spi-B is associated with human precursor B-ALL (14). *Btk* and *Blnk* were found to be targets of PU.1 and Spi-B in our studies, and they are established as tumor suppressors in human precursor B-ALL (36, 42). Expression of the IL-7R has long been known to be a common feature of human childhood or adult B cell leukemia (43, 44). Finally, although IL-7 has been previously suggested to be not required for human B cell development, gain-of-function mutations in the human *IL7R* gene are associated with precursor B-ALL (45, 46). These correlations lead us to expect that further studies using the CD19-CreΔPB mouse model will lead to elucidation of the biochemical pathways that may explain how precursor B-ALL arises in human patients.

Acknowledgments

We thank Kristen Chadwick (London Regional Flow Cytometry Facility) for flow cytometry advice and sorting. We thank David Carter (London Regional Genomics Facility) for assistance and advice with microarray analysis. We acknowledge the University of British Columbia Cancer Research Agency and Genome Quebec for assistance with ChIP sequencing. We thank Dr. C.I. Edvard Smith (Karolinska Institute) for providing the pMSCV-hBTK-FLAG and pMSCV-IRES-GFP retroviral vectors.

Disclosures

The authors have no financial conflicts of interest.

References

1. Ramírez, J., K. Lukin, and J. Hagman. 2010. From hematopoietic progenitors to B cells: mechanisms of lineage restriction and commitment. *Curr. Opin. Immunol.* 22: 177–184.
2. Tijchon, E., J. Havinga, F. N. van Leeuwen, and B. Scheijen. 2013. B-lineage transcription factors and cooperating gene lesions required for leukemia development. *Leukemia* 27: 541–552.
3. Peschon, J. J., P. J. Morrissey, K. H. Grabstein, F. J. Ramsdell, E. Maraskovsky, B. C. Gliniak, L. S. Park, S. F. Ziegler, D. E. Williams, C. B. Ware, et al. 1994. Early lymphocyte expansion is severely impaired in interleukin 7 receptor-deficient mice. *J. Exp. Med.* 180: 1955–1960.
4. Nodland, S. E., M. A. Berkowska, A. A. Bajer, N. Shah, D. de Ridder, J. J. van Dongen, T. W. LeBien, and M. C. van Zelm. 2011. IL-7R expression and IL-7 signaling confer a distinct phenotype on developing human B-lineage cells. *Blood* 118: 2116–2127.
5. Ochiai, K., M. Maienschein-Cline, M. Mandal, J. R. Triggs, E. Bertolino, R. Sciammas, A. R. Dinner, M. R. Clark, and H. Singh. 2012. A self-reinforcing regulatory network triggered by limiting IL-7 activates pre-BCR signaling and differentiation. *Nat. Immunol.* 13: 300–307.
6. Mandal, M., S. E. Powers, K. Ochiai, K. Georgopoulos, B. L. Kee, H. Singh, and M. R. Clark. 2009. Ras orchestrates exit from the cell cycle and light-chain recombination during early B cell development. *Nat. Immunol.* 10: 1110–1117.
7. Mandal, M., S. E. Powers, M. Maienschein-Cline, E. T. Bartom, K. M. Hamel, B. L. Kee, A. R. Dinner, and M. R. Clark. 2011. Epigenetic repression of the *Igk* locus by STAT5-mediated recruitment of the histone methyltransferase Ezh2. *Nat. Immunol.* 12: 1212–1220.
8. Johnson, K., T. Hashimshony, C. M. Sawai, J. M. Pongubala, J. A. Skok, I. Aifantis, and H. Singh. 2008. Regulation of immunoglobulin light-chain recombination by the transcription factor IRF-4 and the attenuation of interleukin-7 signaling. *Immunity* 28: 335–345.
9. Nakayama, J., M. Yamamoto, K. Hayashi, H. Satoh, K. Bundo, M. Kubo, R. Goitsuka, M. A. Farrar, and D. Kitamura. 2009. BLNK suppresses pre-B-cell leukemogenesis through inhibition of JAK3. *Blood* 113: 1483–1492.
10. Sudo, T., S. Nishikawa, N. Ohno, N. Akiyama, M. Tamakoshi, H. Yoshida, and S. Nishikawa. 1993. Expression and function of the interleukin 7 receptor in murine lymphocytes. *Proc. Natl. Acad. Sci. USA* 90: 9125–9129.
11. Ray, D., R. Bosselut, J. Ghysdael, M. G. Mattei, A. Tavitian, and F. Moreau-Gachelin. 1992. Characterization of Spi-B, a transcription factor related to the putative oncoprotein Spi-1/PU.1. *Mol. Cell. Biol.* 12: 4297–4304.
12. DeKoter, R. P., M. Geadah, S. Khoosal, L. S. Xu, G. Thillainadesan, J. Torchia, S. S. Chin, and L. A. Garrett-Sinha. 2010. Regulation of follicular B cell differentiation by the related E26 transformation-specific transcription factors PU.1, Spi-B, and Spi-C. *J. Immunol.* 185: 7374–7384.
13. Mullighan, C. G., J. Zhang, L. H. Kasper, S. Lerach, D. Payne-Turner, L. A. Phillips, S. L. Heatley, L. Holmfeldt, J. R. Collins-Underwood, J. Ma, et al. 2011. CREBBP mutations in relapsed acute lymphoblastic leukaemia. *Nature* 471: 235–239.
14. Fuka, G., M. Kauer, R. Kofler, O. A. Haas, and R. Panzer-Grümayer. 2011. The leukemia-specific fusion gene ETV6/RUNX1 perturbs distinct key biological functions primarily by gene repression. *PLoS ONE* 6: e26348.
15. van der Weyden, L., G. Giotopoulos, A. G. Rust, L. S. Matheson, F. W. van Delft, J. Kong, A. E. Corcoran, M. F. Greaves, C. G. Mullighan, B. J. Huntly, and D. J. Adams. 2011. Modeling the evolution of ETV6-RUNX1-induced B-cell precursor acute lymphoblastic leukemia in mice. *Blood* 118: 1041–1051.
16. Sokalski, K. M., S. K. Li, I. Welch, H. A. Cadieux-Pitre, M. R. Gruca, and R. P. DeKoter. 2011. Deletion of genes encoding PU.1 and Spi-B in B cells impairs differentiation and induces pre-B cell acute lymphoblastic leukemia. *Blood* 118: 2801–2808.
17. Xu, L. S., K. M. Sokalski, K. Hotke, D. A. Christie, O. Zarnett, J. Piskorz, G. Thillainadesan, J. Torchia, and R. P. DeKoter. 2012. Regulation of B cell linker protein transcription by PU.1 and Spi-B in murine B cell acute lymphoblastic leukemia. *J. Immunol.* 189: 3347–3354.
18. Conley, M. E., A. K. Dobbs, D. M. Farmer, S. Kilic, K. Paris, S. Grigoriadou, E. Coustan-Smith, V. Howard, and D. Campana. 2009. Primary B cell immunodeficiencies: comparisons and contrasts. *Annu. Rev. Immunol.* 27: 199–227.
19. Kerner, J. D., M. W. Appleby, R. N. Mohr, S. Chien, D. J. Rawlings, C. R. Maliszewski, O. N. Witte, and R. M. Perlmutter. 1995. Impaired expansion of mouse B cell progenitors lacking Btk. *Immunity* 3: 301–312.
20. Kersseboom, R., S. Middendorp, G. M. Dingjan, K. Dahlenborg, M. Reth, H. Jumaa, and R. W. Hendriks. 2003. Bruton's tyrosine kinase cooperates with the B cell linker protein SLP-65 as a tumor suppressor in pre-B cells. *J. Exp. Med.* 198: 91–98.
21. Winkler, T. H., A. Rolink, F. Melchers, and H. Karasuyama. 1995. Precursor B cells of mouse bone marrow express two different complexes with the surrogate light chain on the surface. *Eur. J. Immunol.* 25: 446–450.
22. Ziliotto, R., M. R. Gruca, S. Podder, G. Noel, C. K. Ogle, D. A. Hess, and R. P. DeKoter. 2014. PU.1 promotes cell cycle exit in the murine myeloid lineage associated with downregulation of E2F1. *Exp. Hematol.* 42: 204–217, e1.
23. Schmittgen, T. D., and K. J. Livak. 2008. Analyzing real-time PCR data by the comparative C(T) method. *Nat. Protoc.* 3: 1101–1108.
24. Cobaleda, C., W. Jochum, and M. Busslinger. 2007. Conversion of mature B cells into T cells by dedifferentiation to uncommitted progenitors. *Nature* 449: 473–477.
25. Johnson, W. E., C. Li, and A. Rabinovic. 2007. Adjusting batch effects in microarray expression data using empirical Bayes methods. *Biostatistics* 8: 118–127.

26. Goecks, J., A. Nekrutenko, and J. Taylor, Galaxy Team. 2010. Galaxy: a comprehensive approach for supporting accessible, reproducible, and transparent computational research in the life sciences. *Genome Biol.* 11: R86.
27. Zhang, Y., T. Liu, C. A. Meyer, J. Eeckhoute, D. S. Johnson, B. E. Bernstein, C. Nusbaum, R. M. Myers, M. Brown, W. Li, and X. S. Liu. 2008. Model-based analysis of ChIP-Seq (MACS). *Genome Biol.* 9: R137.
28. Chen, Y., C. A. Meyer, T. Liu, W. Li, J. S. Liu, and X. S. Liu. 2011. MM-ChIP enables integrative analysis of cross-platform and between-laboratory ChIP-chip or ChIP-seq data. *Genome Biol.* 12: R11.
29. Hardy, R. R., C. E. Carmack, S. A. Shinton, J. D. Kemp, and K. Hayakawa. 1991. Resolution and characterization of pro-B and pre-pro-B cell stages in normal mouse bone marrow. *J. Exp. Med.* 173: 1213–1225.
30. Ito, M., H. Hiramatsu, K. Kobayashi, K. Suzue, M. Kawahata, K. Hioki, Y. Ueyama, Y. Koyanagi, K. Sugamura, K. Tsuji, et al. 2002. NOD/SCID/$\gamma(c)^{null}$ mouse: an excellent recipient mouse model for engraftment of human cells. *Blood* 100: 3175–3182.
31. Ross, M. E., X. Zhou, G. Song, S. A. Shurtleff, K. Girtman, W. K. Williams, H. C. Liu, R. Mahfouz, S. C. Raimondi, N. Lenny, et al. 2003. Classification of pediatric acute lymphoblastic leukemia by gene expression profiling. *Blood* 102: 2951–2959.
32. Turkistany, S. A., and R. P. DeKoter. 2011. The transcription factor PU.1 is a critical regulator of cellular communication in the immune system. *Arch. Immunol. Ther. Exp. (Warsz.)* 59: 431–440.
33. Middendorp, S., G. M. Dingjan, and R. W. Hendriks. 2002. Impaired precursor B cell differentiation in Bruton's tyrosine kinase-deficient mice. *J. Immunol.* 168: 2695–2703.
34. Müller, S., A. Maas, T. C. Islam, P. Sideras, G. Suske, S. Philipsen, K. G. Xanthopoulos, R. W. Hendriks, and C. I. Smith. 1999. Synergistic activation of the human Btk promoter by transcription factors Sp1/3 and PU.1. *Biochem. Biophys. Res. Commun.* 259: 364–369.
35. Müller, S., P. Sideras, C. I. Smith, and K. G. Xanthopoulos. 1996. Cell specific expression of human Bruton's agammaglobulinemia tyrosine kinase gene (Btk) is regulated by Sp1- and Spi-1/PU.1-family members. *Oncogene* 13: 1955–1964.
36. Feldhahn, N., P. Río, B. N. Soh, S. Liedtke, M. Sprangers, F. Klein, P. Wernet, H. Jumaa, W. K. Hofmann, H. Hanenberg, et al. 2005. Deficiency of Bruton's tyrosine kinase in B cell precursor leukemia cells. *Proc. Natl. Acad. Sci. USA* 102: 13266–13271.
37. Gustafsson, M. O., A. Hussain, D. K. Mohammad, A. J. Mohamed, V. Nguyen, P. Metalnikov, K. Colwill, T. Pawson, C. I. Smith, and B. F. Nore. 2012. Regulation of nucleocytoplasmic shuttling of Bruton's tyrosine kinase (Btk) through a novel SH3-dependent interaction with ankyrin repeat domain 54 (ANKRD54). *Mol. Cell. Biol.* 32: 2440–2453.
38. Clark, M. R., M. Mandal, K. Ochiai, and H. Singh. 2014. Orchestrating B cell lymphopoiesis through interplay of IL-7 receptor and pre-B cell receptor signalling. *Nat. Rev. Immunol.* 14: 69–80.
39. Kersseboom, R., V. B. Ta, A. J. Zijlstra, S. Middendorp, H. Jumaa, P. F. van Loo, and R. W. Hendriks. 2006. Bruton's tyrosine kinase and SLP-65 regulate pre-B cell differentiation and the induction of Ig light chain gene rearrangement. *J. Immunol.* 176: 4543–4552.
40. Flemming, A., T. Brummer, M. Reth, and H. Jumaa. 2003. The adaptor protein SLP-65 acts as a tumor suppressor that limits pre-B cell expansion. *Nat. Immunol.* 4: 38–43.
41. Ta, V. B., M. J. de Bruijn, P. J. ter Brugge, J. P. van Hamburg, H. J. Diepstraten, P. F. van Loo, R. Kersseboom, and R. W. Hendriks. 2010. Malignant transformation of Slp65-deficient pre-B cells involves disruption of the Arf-Mdm2-p53 tumor suppressor pathway. *Blood* 115: 1385–1393.
42. Jumaa, H., L. Bossaller, K. Portugal, B. Storch, M. Lotz, A. Flemming, M. Schrappe, V. Postila, P. Riikonen, J. Pelkonen, et al. 2003. Deficiency of the adaptor SLP-65 in pre-B-cell acute lymphoblastic leukaemia. *Nature* 423: 452–456.
43. De Waele, M., W. Renmans, K. Vander Gucht, K. Jochmans, R. Schots, J. Otten, F. Trullemans, P. Lacor, and I. Van Riet. 2001. Growth factor receptor profile of $CD34^+$ cells in AML and B-lineage ALL and in their normal bone marrow counterparts. *Eur. J. Haematol.* 66: 178–187.
44. Sasson, S. C., S. Smith, N. Seddiki, J. J. Zaunders, A. Bryant, K. K. Koelsch, C. Weatherall, M. L. Munier, C. McGinley, J. Yeung, et al. 2010. IL-7 receptor is expressed on adult pre-B-cell acute lymphoblastic leukemia and other B-cell derived neoplasms and correlates with expression of proliferation and survival markers. *Cytokine* 50: 58–68.
45. Shochat, C., N. Tal, O. R. Bandapalli, C. Palmi, I. Ganmore, G. te Kronnie, G. Cario, G. Cazzaniga, A. E. Kulozik, M. Stanulla, et al. 2011. Gain-of-function mutations in interleukin-7 receptor-α (IL7R) in childhood acute lymphoblastic leukemias. *J. Exp. Med.* 208: 901–908.
46. Kim, M. S., N. G. Chung, M. S. Kim, N. J. Yoo, and S. H. Lee. 2013. Somatic mutation of IL7R exon 6 in acute leukemias and solid cancers. *Hum. Pathol.* 44: 551–555.